

Heterogeneous Sheaf Neural Networks

Luke Braithwaite^{1*}, Iulia Duta¹, Pietro Liò¹

¹Department of Computer Science and Technology, University of Cambridge

Abstract

Heterogeneous graphs, with nodes and edges of different types, are commonly used to model relational structures in many real-world applications. Standard Graph Neural Networks (GNNs) struggle to process heterogeneous data due to oversmoothing. Instead, current approaches have focused on accounting for the heterogeneity in the model architecture, leading to increasingly complex models. Inspired by recent work, we propose using cellular sheaves to model the heterogeneity in the graph’s underlying topology. Instead of modelling the data as a graph, we represent it as cellular sheaves, which allows us to encode the different data types directly in the data structure, eliminating the need to inject them into the architecture. We introduce HETSHEAF, a general framework for heterogeneous sheaf neural networks, and a series of heterogeneous sheaf predictors to better encode the data’s heterogeneity into the sheaf structure. Finally, we empirically evaluate HETSHEAF on several standard heterogeneous graph benchmarks, achieving competitive results whilst being more parameter-efficient.

1 Introduction

Heterogeneous graphs with node and edge types [23, 11, 47] are commonly found in many real-world applications such as protein prediction [15], recommendation systems [13, 49], social network analysis [32, 26] and traffic prediction [18]. Lv et al. [28] surveyed different approaches for processing heterogeneous graph data. Standard Graph Neural Networks (GNNs) struggle to process heterogeneous data due to *oversmoothing*. This is where neighbouring nodes have increasingly similar representations as the message passing process continues, particularly in deeper GNNs with multiple message passing layers. In the case of heterogeneous graphs and hypergraphs, this causes all of the type-specific features and information to be lost during the message passing process, significantly reducing the model’s performance.

Existing heterogeneous GNNs (HGNNs) [34, 51, 24, 43] represent the data as a simple graph and attempt to account for the heterogeneity only in the model architecture. Recent literature [4, 3, 12, 2] has demonstrated that attaching a *cellular sheaf* [9, 36] to a standard graph helps mitigate oversmoothing and increases the expressivity. While sheaf structure is beneficial for homogeneous graphs, we argue that its structure becomes even more essential in heterogeneous setups, where different node and edge representations are inherently situated in distinct feature spaces. However, the use of sheaf-based methods to model heterogeneous data remained unexplored.

Compared to a standard graph, the sheaf assigns a vector space to each node and edge in the graph, together with a mechanism that allows communication between these spaces. This means that each edge and node can have completely different local meanings if they can be connected to create a meaningful global representation. Put differently, the sheaf can implicitly model the heterogeneity in the data. This means the model architecture is no longer required to account for or model the data’s heterogeneity. The sheaf handles it for us. We take advantage of this observation to propose **HETSHEAF** — a sheaf-based framework for heterogeneous data, which learns to infer a cellular

*Corresponding author: lb2027@cam.ac.uk

sheaf that encodes all the necessary information about the heterogeneous data. By using data structures that properly incorporate all the type-specific information, we eliminate the need for domain-specific architectural design.

Contributions. Our main contributions may be summarised as follows:

1. We propose **HETSHEAF**, a general framework for creating heterogeneous sheaf neural networks. Unlike existing models, which focus on tweaking the neural network architectures to account for the heterogeneity of the data, our model uses cellular sheaves to incorporate all the type-specific information and can be further processed with any existing architecture designed for sheaf data.
2. We demonstrate the benefit of modelling heterogeneous data using Sheaf Graph Neural Networks on a series of heterogeneous datasets. These techniques are *competitive against existing approaches and achieve state-of-the-art results on several benchmarks, with a clear advantage in terms of model size.*
3. We introduce a series of novel **heterogeneous sheaf predictors** demonstrating how the sheaf’s restriction maps may be modified to account for the type of information encoded in the heterogeneous data.

2 Related Work

Homogeneous GNNs. Many different homogeneous GNNs have been proposed [20, 25, 27, 41], all of which can process heterogeneous graphs by ignoring the node/edge types. Graph Convolutional Networks (GCNs) [25] approximate spectral convolutional neural networks [10], by restricting the processing to first-order neighbourhoods. To enable a more expressive neighbourhood aggregation, Graph Attention Networks (GATs) [41] use a self-attention mechanism similar to the one used in transformers [40], while Principal Neighbourhood Aggregation (PNA) [8] combines multiple aggregators leading to provably more expressive architectures.

Sheaf GNNs. However, standard GNNs suffers from limitations such as oversmoothing [5] or oversquashing [1]. To alleviate them, geometric structure in the form of cellular sheaves was incorporated, leading to neural sheaf diffusion [4]. Recent work has extended upon the original sheaf diffusion to include an attention mechanism [3], positional encoding [22] and a connection laplacian [2]. As well as extending to hypergraph domains [12] and applied to recommendation systems [31].

Heterogeneous GNNs. Compared to homogeneous graphs where all nodes/edges encodes the same type of data, in heterogeneous graphs nodes and edges can represents different types of information. In order to process them, various heterogeneous graph neural networks (HGNNs) were proposed. Some HGNNs use *meta-paths* [39, 38], pre-defined node or edge type patterns that aim to capture important semantic information. HAN [44] uses a hierarchical attention mechanism to capture node-level importance between nodes and semantic-level importance between meta-paths. MAGNN [16] combines several meta-path encoders to aggregate all information along the meta-path. Both HAN and MAGNN require meta-paths to be manually generated beforehand. Graph Transformer Networks (GTNs) [50] automate this process by learning meta-paths with graph transformation layers. Meta-paths are expensive to compute, so they are infeasible in graphs with many different edge types. Instead, the graph may be treated as a relational graph.

RSHN [54] builds a coarsened line graph to generate edge features, then applies a Message Passing Neural Network (MPNN) [17] to propagate the node and edge features. R-GCN [35] splits the heterogeneous graph into the subgraph induced by each edge type, then applies a standard GCN to each subgraph. HGT [51] is a graph transformer that can process large heterogeneous graphs using subgraph sampling. HetGNN [51] uses random walks to sample strongly correlated heterogeneous neighbours and then applies an RNN for representation learning. SlotGAT [53] uses a slot-based message passing approach with an attention mechanism for aggregation. Finally, simple-HGNN [28], which applies a series of additional techniques to lift GATs to heterogeneous domains and Space4HGNN [52] defines a unified design space of modular components for heterogeneous GNNs and allows exhaustive evaluation of many combinations of techniques. Instead of introducing a new architecture for heterogeneous graphs, we propose to shift from representing heterogeneous relational data as graphs to cellular sheaves, which preserve all the type-specific information and

enable a powerful processing through sheaf-specific tools. Moreover, we introduce a set of sheaf predictors conditioned on the type-information, to properly encode the necessary information.

3 Preliminaries

We briefly overview the necessary background, starting with heterogeneous graphs and cellular sheaf theory and concluding with neural sheaf diffusion. Refer to Curry [9] or Rosiak [33] for a more in-depth discussion of cellular sheaf theory, and Bodnar et al. [4] for the full theoretical results of neural sheaf diffusion.

Heterogeneous Graphs. A heterogeneous graph [38] is $\mathcal{G} = (\mathcal{V}, \mathcal{E}, \phi, \psi)$ where \mathcal{V} is a set of nodes, \mathcal{E} is a set of edges, ϕ is a node type mapping function and ψ is an edge type mapping function. Each node u has a type $\phi(u)$ and each edge $e := (u, v)$ has a type $\psi(e)$, also denoted $\psi(u, v)$. Let Φ and Ψ be the sets of all node and edge types in \mathcal{G} , respectively. Assume that each node type in Φ is represented by a consecutive integer starting from 0 with the t denoting the t -th node type. An identical representation is used for the edge types.

Each node u has a feature vector \mathbf{x}_u . For each node type $t \in \Phi$, the type- t nodes $\{u \in \mathcal{V} \mid \phi(u) = t\}$ have the same feature dimension $d_0^t = d_0^{\phi(u)}$ i.e. $\mathbf{x}_u \in \mathbb{R}^{d_0^{\phi(u)}}$. Different node types may have different feature dimensions.

Cellular Sheaves. Intuitively, sheaves “glue” local data assignments together to form a consistent global representation or data assignment. In the case of graphs, these local data assignments are the feature vectors assigned to each node/edge, which are then connected together by defining a series of linear maps that connect the latent spaces in which each of these node features lives.

Definition 1. A *cellular sheaf* $(\mathcal{G}, \mathcal{F})$ attached to an undirected graph $\mathcal{G} = (\mathcal{V}, \mathcal{E})$ is defined as a triple $\langle \mathcal{F}(u), \mathcal{F}(e), \mathcal{F}_{u \trianglelefteq e} \rangle$ consisting of:

- *Node stalks* $\mathcal{F}(u)$: a vector space associated with each vertex $u \in \mathcal{V}$.
- *Edge stalks* $\mathcal{F}(e)$: a vector space for each edge $e \in \mathcal{E}$.
- *Linear restriction maps* $\mathcal{F}_{u \trianglelefteq e} : \mathcal{F}(u) \rightarrow \mathcal{F}(e)$ for each incident node-edge pair $u \trianglelefteq e$.

The space formed by the node stalks is known as the space of 0-cochains $C^0(\mathcal{G}, \mathcal{F}) := \bigoplus_{u \in \mathcal{V}} \mathcal{F}(u)$, and the space formed by the edge stalks is the space of 1-cochains $C^1(\mathcal{G}, \mathcal{F}) := \bigoplus_{e \in \mathcal{E}} \mathcal{F}(e)$.

The spaces $C^0(\mathcal{G}, \mathcal{F})$ and $C^1(\mathcal{G}, \mathcal{F})$ construct the *co-boundary map* $\delta : C^0(\mathcal{G}, \mathcal{F}) \rightarrow C^1(\mathcal{G}, \mathcal{F})$ which is defined edgewise as $\delta(\mathbf{x})_e := \mathcal{F}_{v \trianglelefteq e} \mathbf{x}_v - \mathcal{F}_{u \trianglelefteq e} \mathbf{x}_u$, given an arbitrary edge direction $e = u \rightarrow v$. Hansen and Ghrist [21] provide an opinion dynamics interpretation for each object. The node stalk $\mathcal{F}(u)$ represents the “private opinion” of the node u and $\mathcal{F}_{u \trianglelefteq e} \mathbf{x}_u$ is how the opinion is expressed in the public “discourse space” formed by the edge stalk $\mathcal{F}(e)$. The co-boundary map δ measures the disagreement between nodes and may be used to define the sheaf Laplacian, which measures the aggregated disagreement at each node.

Definition 2. The *sheaf Laplacian* of a sheaf $(\mathcal{G}, \mathcal{F})$ is defined as $L_{\mathcal{F}} := \delta^\top \delta$ and can be defined node-wise as

$$L_{\mathcal{F}}(\mathbf{x})_u = \sum_{u, v \trianglelefteq e} \mathcal{F}_{u \trianglelefteq e}^\top (\mathcal{F}_{u \trianglelefteq e} \mathbf{x}_u - \mathcal{F}_{v \trianglelefteq e} \mathbf{x}_v). \quad (1)$$

The sheaf Laplacian is a positive semi-definite block matrix with block diagonals of $L_{\mathcal{F}_{uu}} = \sum_{u \trianglelefteq e} \mathcal{F}_{u \trianglelefteq e}^\top \mathcal{F}_{u \trianglelefteq e}$ and off-diagonal blocks $L_{\mathcal{F}_{uv}} = -\mathcal{F}_{u \trianglelefteq e}^\top \mathcal{F}_{v \trianglelefteq e}$. The *normalised sheaf Laplacian* is given by $\Delta_{\mathcal{F}} := D^{-1/2} L_{\mathcal{F}} D^{-1/2}$ where D is the block diagonal of $L_{\mathcal{F}}$.

Unless otherwise stated, we assign the same d -dimensional space to each stalk, that is $\mathcal{F}(u) = \mathbb{R}^d$ and $\mathcal{F}(e) = \mathbb{R}^d$ where d is the *dimension* of the stalk. This means that the sheaf Laplacian has the dimensions of $dn \times dn$. Assuming a trivial sheaf, all stalks are \mathbb{R} , and all restriction maps are the identity, we recover the standard graph Laplacian.

Neural Sheaf Diffusion. Consider an undirected graph $\mathcal{G} = (\mathcal{V}, \mathcal{E})$ where each node $u \in \mathcal{V}$ has a d -dimensional feature vector $\mathbf{x}_u \in \mathcal{F}(u)$. The nd -dimensional column vector $\mathbf{x} \in C^0(\mathcal{G}, \mathcal{F})$ is constructed by stacking the individual node feature vectors \mathbf{x}_u . If we allow for up to f feature channels,

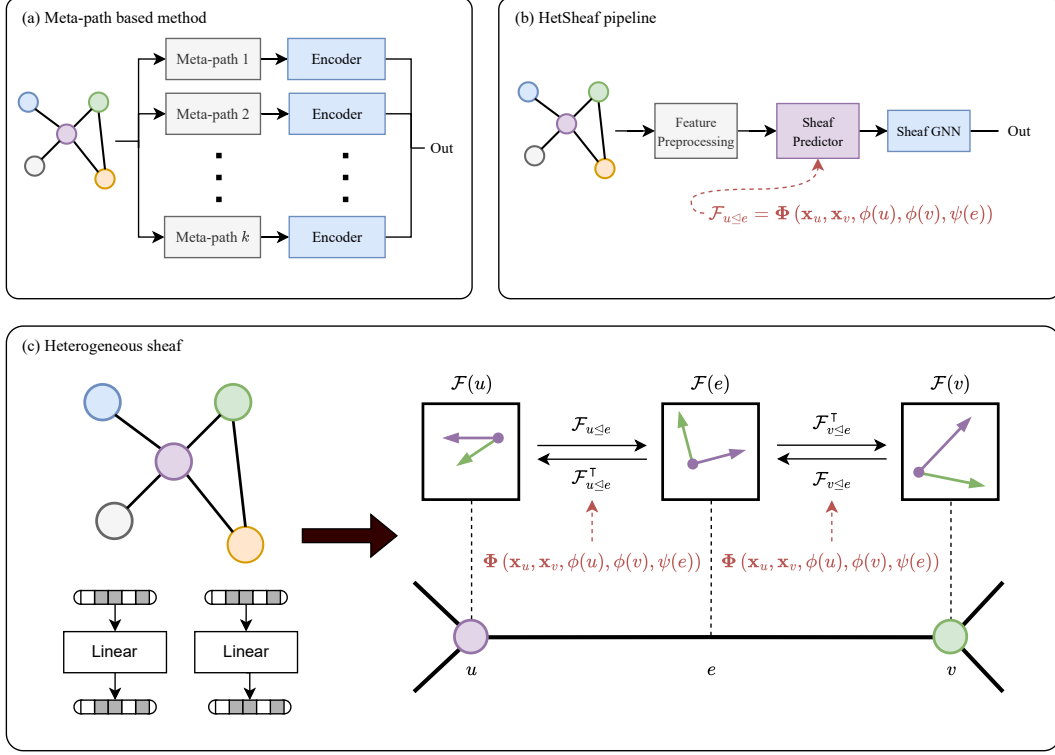


Figure 1: **HETSHEAF: a sheaf-based framework for heterogeneous data.** (a) In the **standard meta-path approach for heterogeneous GNN**, a series of domain-specific meta-paths are extracted from the original heterogeneous graph and then fed into an encoder to generate the latent representations. (b) This is in contrast to the **HETSHEAF pipeline**, which uses a sheaf to capture the underlying heterogeneity. First, the node features are preprocessed by projecting them into the same number of input channels using a linear layer. The resulting features are used to infer the sheaf structure: the nodes are projected into their respective node stalks, and the restriction maps are predicted as described in section 4.2. Compared to a standard graph, this structure already encompasses all the necessary information about the heterogeneous structure, eliminating the need for handcrafted architectures. The predicted sheaf is further processed using any SheafGNN method. (c) **Learning heterogeneous sheaves.** In the sheaf predictor, the node features are enriched with information about the nodes and edge type, to infer a sheaf structure conditioned on the heterogeneous information.

we have the feature matrix $\mathbf{X} \in \mathbb{R}^{nd \times f}$ where each column represents a vector in $C^0(\mathcal{G}, \mathcal{F})$ for its corresponding feature channel.

Sheaf diffusion is a diffusion process on $(\mathcal{G}, \mathcal{F})$ that modifies the standard graph diffusion process [25, 7]. Bodnar et al. [4] used the modified discrete diffusion process

$$\mathbf{X}^{(t+1)} = \mathbf{X}^{(t)} - \sigma \left(\Delta_{\mathcal{F}(t)} \left(\mathbf{I}_{nd} \otimes \mathbf{W}_1^{(t)} \right) \mathbf{X}^{(t)} \mathbf{W}_2^{(t)} \right). \quad (2)$$

where \mathbf{W}_1 and \mathbf{W}_2 are weight matrices and the restriction maps defining $\Delta_{\mathcal{F}(t)}$ are computed using the parametric matrix-valued function $\mathcal{F}_{u \leq e := (u,v)} = \Phi(\mathbf{x}_u, \mathbf{x}_v) = \text{MLP}(\mathbf{x}_u \parallel \mathbf{x}_v)$ where \parallel denotes vector concatenation. This is known as *Neural Sheaf Diffusion* (NSD).

4 Sheaves for Heterogeneous Data

4.1 Why Sheaves?

Existing heterogeneous GNN architectures (fig. 1a) seek to account for the data heterogeneity explicitly in the model architecture. This results in a series of shortcomings. Since standard architectures are unaware of node/edge types, additional research effort is required to develop models specially designed for heterogeneous data. This usually translates into increased model complexity, with a number of parameters that scale with the entity types. Moreover, the resulting tools lack interpretability and are hard to analyse theoretically.

On the other hand, instead of modifying the architecture, we propose to modify the input structure to encode specific heterogeneous knowledge while maintaining topological information. We assert that a cellular sheaf is ideal for this purpose, offering all the necessary tools to model interactions between non-homogeneous data. Additionally, we propose a series of modifications to the original sheaf inference models to incorporate the heterogeneous information more explicitly. The resulting data structure can be modelled using existing sheaf neural networks, enabling the use of all sheaf-related mathematical tools to analyze the message passing processing on the heterogeneous graph.

Standard graphs have associated a feature space S , with each node u having a vector representation \mathbf{x}_u from that space $\mathbf{x}_u \in S$. This is suitable for homogeneous data, where all nodes contain the same type of information. However, it becomes unnatural when heterogeneous information is provided. In a heterogeneous setup, a standard graph representation would enforce all the distinct node-specific spaces to be encoded in the same space S . Contrary, sheaves assign cochains $C^0(\mathcal{G}, \mathcal{F}) := \bigoplus_{u \in \mathcal{V}} \mathcal{F}(u)$, with a distinct space $\mathcal{F}(u)$ attached to each node in the graph and restriction maps that help to learn common “communication tunnels” between these spaces. The restriction maps allows us to communicate between different kind of information, while preserving the uniqueness of each type. This suggests a strong alignment between the sheaf principles and the heterogeneous requirements. Taking this into account, instead of tweaking another architecture for heterogeneous data, we propose switching from the classical graph representation framework towards sheaf representation learning for heterogeneous problems, which we show to be beneficial both in terms of performance and memory efficiency.

4.2 Heterogeneous Sheaf Predictors

Without an oracle sheaf structure, previous works using sheaf neural networks for graph data learn to predict the sheaf from the node features $\mathcal{F}_{u \triangleleft (u,v)} = \Phi(\mathbf{x}_u, \mathbf{x}_v)$.

Although, given enough data, a sheaf can learn different propagation mechanisms for different nodes, it doesn’t explicitly encodes the type information. As this information is available for heterogeneous data, its inclusion may help yield more expressive representations and allow the model to learn the inter-type communication tunnels more easily. With this in mind, we propose modifying the sheaf parameterisation to *explicitly* account for the type information (fig. 1c). This yields the modified restriction map parameterisation:

$$\mathcal{F}_{u \triangleleft e := (u,v)} = \Phi(\mathbf{x}_u, \mathbf{x}_v, \phi(u), \phi(v), \psi(e)). \quad (3)$$

We propose a series *heterogeneous sheaf predictors* based on the parameterisation in eq. (3) to account for the type information explicitly and a modified version of the neural sheaf diffusion restriction map parameterisation. Similar to Bodnar et al. [4], we experiment with three different restriction map types: diagonal, orthogonal and general.

The first approach embeds the type information as additional features in the node and edge feature vectors. As the types are numeric, they are encoded as a one-hot vector before they are embedded. The most straightforward approach is concatenating the one-hot encoded type vectors to the existing feature vectors. Let \mathcal{G} be a heterogeneous graph, with features $\mathbf{x}_u \in \mathbb{R}^f$ associated with each node $u \in \mathcal{V}$, $\mathbf{e}_{\phi(u)}$ be the one-hot encoded node type associated with node u , $\mathbf{e}_{\psi(e)}$ be one-hot encoded edge type associated with the edge $e := (u, v)$ and \parallel denote vector concatenation.

HetSheaf-TE. Naïvely, the simplest approach would be to concatenate all the type information and the local features. This leads to the following restriction map formulation

$$\mathcal{F}_{u \triangleleft e} := \text{MLP}(\mathbf{x}_u \parallel \mathbf{x}_v \parallel \mathbf{e}_{\phi(u)} \parallel \mathbf{e}_{\phi(v)} \parallel \mathbf{e}_{\psi(e)}). \quad (4)$$

This formulation’s benefit is that it explicitly accounts for all available type information, so it should, in theory, be better able to model the heterogeneity in the data than the neural sheaf diffusion sheaf predictor. However, this approach is computationally wasteful in either node heterogeneity with edge homogeneity or edge heterogeneity with node homogeneity, as the model includes redundant type information that increases the number of training parameters and could increase the chance of overfitting. This could similarly apply in cases where the edge type encodes the types of connected nodes, as the edge type is redundant and can be easily inferred from the node types. It may be more sensible to embed only the salient type information instead of all available type information.

HetSheaf-EE. This modifies HetSheaf-TE by embedding only the edge type information, giving restriction maps formulated as

$$\mathcal{F}_{u \trianglelefteq e} := \text{MLP}(\mathbf{x}_u \parallel \mathbf{x}_v \parallel \mathbf{e}_{\psi(e)}), \quad (5)$$

which provides a more natural formulation when only the graph edges are heterogeneous and is more efficient in terms of model parameters. The main downside is losing some generality and flexibility in the final computed sheaf.

HetSheaf-NE. Likewise, if the graph is heterogeneous only across its nodes, embedding just the node types is more natural. This yields restriction maps formulated as

$$\mathcal{F}_{u \trianglelefteq e} := \text{MLP}(\mathbf{x}_u \parallel \mathbf{x}_v \parallel \mathbf{e}_{\phi(u)} \parallel \mathbf{e}_{\phi(v)}). \quad (6)$$

The benefits and drawbacks of this formulation are identical to those of HetSheaf-EE.

Additionally, we may learn restriction maps that include only the type information and not the local information, allowing us to test the relative importance of the type information compared to the local node features.

HetSheaf-types. The natural starting point is to embed all available type information such that

$$\mathcal{F}_{u \trianglelefteq e} := \text{MLP}(\mathbf{e}_{\phi(u)} \parallel \mathbf{e}_{\phi(v)} \parallel \mathbf{e}_{\psi(e)}). \quad (7)$$

This approach’s benefits and drawbacks are similar to HetSheaf-TE’s, whilst requiring substantially fewer parameters than HetSheaf-TE, HetSheaf-NE, or HetSheaf-EE. This is, of course, assuming that $|\Phi|, |\Psi| \ll f$, which is a reasonable assumption in most settings. The main drawback compared to including the local features is that the learnt sheaf is likely unable to account for them and will likely perform worse than HetSheaf-NSD or any previous approaches. As with HetSheaf-TE, HetSheaf-types may be modified to account for setups in which only the nodes or edges are heterogeneous.

HetSheaf-ET. This approach is more natural when only the edges of the graphs are heterogeneous and is a modified version of HetSheaf-EE. Its restriction maps are defined as

$$\mathcal{F}_{u \trianglelefteq e} := \text{MLP}(\mathbf{e}_{\phi(e)}). \quad (8)$$

HetSheaf-NT. Finally, the restriction maps can include only the node type information, which may be useful in cases when only the nodes of the graphs are heterogeneous. The restriction maps are defined as

$$\mathcal{F}_{u \trianglelefteq e} := \text{MLP}(\mathbf{e}_{\phi(u)} \parallel \mathbf{e}_{\phi(v)}). \quad (9)$$

The key drawback of simply embedding the type information is that the same MLP is used for different edge types. This implicitly assumes that the same mechanism generates the restriction maps across each edge type. The benefit of sheaves is that they can learn a different message passing mechanism for each different node or edge type through the restriction maps, so the type embedding approaches do not fully exploit this benefit. Instead, the sheaf should be able to generate the restriction maps for each edge type using a different mechanism.

HetSheaf-ensemble. This uses a different MLP for each edge type. More formally, the restriction maps may be formulated as

$$\mathcal{F}_{u \trianglelefteq e} := \text{MLP}_{\psi(e)}(\mathbf{x}_u \parallel \mathbf{x}_v) \quad (10)$$

where $\psi(e)$ is the edge type associated with the edge $e := (u, v)$. This approach may also be augmented by concatenating the node types. The benefit of this approach is that a separate generation mechanism is used for each edge type, so it will be more expressive than reusing the same MLP across each edge type. However, it has a significant downside: it causes a substantial increase in the number of model parameters, which greatly increases the computational overhead in terms of training time and memory usage. This could be a major issue with larger datasets, as the size of GPU memory could make this approach infeasible.

Table 1: **Performance on heterogeneous node classification.** Results of the heterogeneous sheaf learners and baselines from the literature are shown. The average macro and micro F1 score and standard deviation after 10 runs. The top three models are coloured by **First**, **Second** and **Third**.

	ACM		DBLP		IMDB	
	Macro F1	Micro F1	Macro F1	Micro F1	Macro F1	Micro F1
GAT	75.8 ± 10.7	77.91 ± 8.66	95.47 ± 0.44	95.70 ± 0.42	84.12 ± 0.96	85.31 ± 0.92
GCN	89.09 ± 3.66	89.14 ± 3.60	96.31 ± 0.73	96.57 ± 0.63	82.41 ± 1.15	83.99 ± 0.92
HAN	86.95 ± 6.19	86.64 ± 6.43	94.74 ± 0.81	95.01 ± 0.73	13.53 ± 0.24	38.70 ± 1.13
R-GCN	95.81 ± 0.39	95.75 ± 0.39	96.79 ± 0.39	97.01 ± 0.34	88.16 ± 0.67	89.08 ± 0.63
HGT	93.24 ± 3.19	93.30 ± 2.91	93.91 ± 1.08	94.26 ± 1.09	87.74 ± 0.76	88.45 ± 0.71
HetSheaf-NSD	94.97 ± 0.41	94.94 ± 0.42	96.69 ± 0.82	96.89 ± 0.79	86.70 ± 0.90	87.50 ± 0.78
HetSheaf (ours)	96.39 ± 0.37	96.35 ± 0.36	97.93 ± 0.36	98.08 ± 0.31	87.12 ± 0.75	87.88 ± 0.67

4.3 HETSHEAF: A General Heterogeneous Sheaf Neural Network Framework

Figure 1b illustrates the final HETSHEAF pipeline. After the input features are preprocessed, we project them into their respective stalk spaces using an MLP. The restriction maps are generated using a heterogeneous sheaf predictor (Section 4.2). After the new heterogeneous sheaf is fed into a Sheaf GNN architecture, which, in our case, is a neural sheaf diffusion model, the postprocessed latent representations are used as input for the final downstream decoder. We briefly describe the feature preprocessing and postprocessing in more detail.

Feature preprocessing. As each node type may have a different number of feature channels, we use a linear layer with bias for each node type to project the node features to the same number of input channels. The weights of these linear layers are optimised as part of the training process. This can be combined with the sheaf projection step of the SheafGNN to create the sheaf cochain $\mathbf{x} \in C^0(\mathcal{G}, \mathcal{F})$. The modified linear layer takes in the original feature channels f_0 and outputs df features as the node stalk projection. We follow Lv et al. [28], Zhou et al. [53] to generate the input feature types by using either all of the node feature types (type-0), only the feature of the node target type (type-1) or replacing all node features as one-hot vectors (type-2).

Postprocessing. Similar to Lv et al. [28], we perform ℓ_2 normalisation on the output embedding,

$$\mathbf{o}_u = \frac{\mathbf{h}_u^{(L)}}{\|\mathbf{h}_u^{(L)}\|}, \quad (11)$$

where \mathbf{o}_u is the final output embedding for a node $u \in \mathcal{V}$ and $\mathbf{h}_u^{(L)}$ is the final hidden representation from the SheafGNN. For link prediction, we adapt JKNet [45] to create the final embedding by concatenating the hidden representations for each layer, i.e.

$$\mathbf{o}_u = \left\| \frac{\mathbf{h}_u^{(l)}}{\|\mathbf{h}_u^{(l)}\|} \right\|_{l=1}^L. \quad (12)$$

5 Experiments

5.1 Experimental Setup

Datasets. Table 5 shows the statistics of a series of widely used heterogeneous benchmark datasets [28, 53, 43, 24, 48]. The datasets cover node classification and link prediction tasks across various domains, including citation graphs (e.g., DBLP, ACM) and knowledge graphs (e.g., IMDB, LastFM, MovieLens). Appendix A.1.1 contains descriptions of each dataset.

Baselines. We compare against GAT [42], GCN [25], HAN [44], HGT [24], R-GCN [34] and Neural Sheaf Diffusion [4].

Evaluation setup. For node classification, the target node labels were split with 1000 labels for testing, 500 for validation, and the remaining for training. For link prediction, the data is split using the ratio 81 % : 9 % : 10 % for training, validation and testing, respectively. Each experiment is

Table 2: **Performance on heterogeneous link prediction benchmarks.** Results for the heterogeneous sheaf learners and baselines are shown. The table shows the average and standard deviation of the binary AUROC and AUPR scores after 10 runs with the top three models, coloured **First**, **Second** and **Third**. The runs labelled “OOM” were caused by an out-of-memory error of the GPU.

	LastFM		MovieLens	
	AUPR	AUROC	AUPR	AUROC
GAT	62.88 \pm 0.18	50.69 \pm 0.63	97.06 \pm 0.24	97.47 \pm 0.21
GCN	96.84 \pm 0.10	96.42 \pm 0.08	99.57 \pm 0.03	99.51 \pm 0.03
HAN	82.48 \pm 3.86	78.47 \pm 3.04	63.49 \pm 0.14	52.06 \pm 0.27
R-GCN	96.86 \pm 0.07	96.97 \pm 0.05	99.06 \pm 0.05	99.13 \pm 0.04
HGT	OOM	OOM	OOM	OOM
HetSheaf-NSD	97.16 \pm 0.19	96.58 \pm 0.18	99.66 \pm 0.04	99.57 \pm 0.03
HetSheaf (ours)	98.24 \pm 0.13	97.80 \pm 0.18	99.68 \pm 0.04	99.59 \pm 0.04

Table 3: **Ablation study of the impact of different restriction maps and sheaf predictor types on node classification performance.** The highest performing restriction map type for each sheaf learner is highlighted, and the highest performing sheaf learner is shown in **bold**.

	ACM		DBLP		IMDB	
	Macro F1	Micro F1	Macro F1	Micro F1	Macro F1	Micro F1
O(d)-NSD	94.64 \pm 1.02	94.59 \pm 1.03	96.32 \pm 0.46	96.55 \pm 0.42	86.35 \pm 1.29	87.20 \pm 1.07
Diag-NSD	94.42 \pm 0.51	94.42 \pm 0.48	95.25 \pm 0.70	95.52 \pm 0.67	86.36 \pm 0.94	87.26 \pm 0.78
Gen-NSD	94.97 \pm 0.41	94.94 \pm 0.42	96.69 \pm 0.82	96.89 \pm 0.79	86.70 \pm 0.90	87.50 \pm 0.78
O(d)-TE	95.04 \pm 0.73	95.00 \pm 0.76	96.13 \pm 0.74	96.37 \pm 0.73	86.32 \pm 0.90	87.09 \pm 0.68
Diag-TE	95.74 \pm 0.86	95.74 \pm 0.83	97.16 \pm 0.64	97.36 \pm 0.62	86.32 \pm 0.71	87.07 \pm 0.61
Gen-TE	96.11 \pm 0.49	96.09 \pm 0.51	97.93 \pm 0.36	98.08 \pm 0.31	86.85 \pm 0.81	87.67 \pm 0.80
O(d)-ensemble	94.99 \pm 1.23	95.00 \pm 1.21	96.31 \pm 0.63	96.52 \pm 0.59	86.16 \pm 0.71	87.03 \pm 0.62
Diag-ensemble	95.89 \pm 0.68	95.89 \pm 0.67	96.92 \pm 0.91	97.09 \pm 0.89	86.62 \pm 0.91	87.45 \pm 0.82
Gen-ensemble	96.16 \pm 0.52	96.12 \pm 0.54	97.46 \pm 0.64	97.62 \pm 0.60	86.92 \pm 1.10	87.79 \pm 0.95
O(d)-NE	94.65 \pm 0.99	94.64 \pm 0.96	96.55 \pm 0.56	96.69 \pm 0.54	86.38 \pm 0.93	87.11 \pm 1.02
Diag-NE	94.94 \pm 0.60	94.90 \pm 0.59	97.01 \pm 0.71	97.22 \pm 0.67	86.87 \pm 1.01	87.73 \pm 0.81
Gen-NE	96.13 \pm 0.39	96.09 \pm 0.38	97.68 \pm 0.55	97.83 \pm 0.51	86.54 \pm 0.71	87.46 \pm 0.74
O(d)-EE	95.00 \pm 0.80	95.00 \pm 0.79	96.51 \pm 0.64	96.73 \pm 0.56	87.12 \pm 0.75	87.88 \pm 0.67
Diag-EE	95.09 \pm 0.51	95.05 \pm 0.51	96.86 \pm 0.47	97.07 \pm 0.47	85.99 \pm 0.63	86.85 \pm 0.58
Gen-EE	96.39 \pm 0.37	96.35 \pm 0.36	97.57 \pm 0.69	97.73 \pm 0.62	86.60 \pm 0.93	87.51 \pm 0.92
O(d)-NT	94.30 \pm 1.10	94.28 \pm 1.12	96.63 \pm 0.44	96.78 \pm 0.42	86.35 \pm 1.04	87.26 \pm 0.94
Diag-NT	94.98 \pm 0.58	94.96 \pm 0.60	96.96 \pm 0.41	97.11 \pm 0.36	85.85 \pm 1.07	86.78 \pm 0.91
Gen-NT	96.12 \pm 0.36	96.12 \pm 0.32	97.88 \pm 0.47	98.04 \pm 0.43	86.92 \pm 0.95	87.76 \pm 0.85
O(d)-ET	94.37 \pm 1.35	94.32 \pm 1.37	96.15 \pm 0.46	96.33 \pm 0.46	85.92 \pm 0.68	87.01 \pm 0.57
Diag-ET	95.44 \pm 0.37	95.40 \pm 0.38	97.34 \pm 0.56	97.55 \pm 0.49	85.96 \pm 0.74	86.90 \pm 0.69
Gen-ET	95.84 \pm 0.65	95.82 \pm 0.65	97.69 \pm 0.47	97.83 \pm 0.47	86.12 \pm 0.82	87.05 \pm 0.69

repeated on 10 random splits for each dataset, with the average and standard deviation reported. For node classification, we report the micro-average and macro-averaged F1 scores. We report the mean reciprocal rank (MRR) and the ROC-AUR for link prediction. The negative test samples for link prediction are generated randomly [16, 51, 6].

5.2 Experimental Results

Node classification. Table 1 reports the node classification results on three benchmark datasets, with the mean Macro-F1 and Micro-F1 and their standard deviation reported. The overall trend is that HetSheaf achieves competitive results across all datasets and state-of-the-art performance on both ACM and DBLP. For instance, on ACM, the Micro F1 score is 96.35 %, while that of the best

competitor is 95.81 %; moreover, HetSheaf has a smaller standard deviation 0.37, compared to 0.39 of its competitor. On IMDB, HetSheaf obtains comparable results with both R-GCN and HGT with a Micro F1 score of 87.88 % compared to 88.45 of HGT and 89.09 % of R-GCN, with a much smaller parameter budget (see Table 7). The superior performance of HetSheaf on the node classification suggests that the sheaf can learn richer representations to preserve node heterogeneity in the various benchmark datasets.

Link prediction. Table 2 reports the link prediction results on LastFM and MovieLens, with the mean AUROC and AUPR and their standard deviation reported. HetSheaf achieves the best performance on both datasets and both metrics. For instance, on LastFM, HetSheaf achieves an AUROC of 87.80 %, which is 1.22 % higher than HetSheaf-NSD, the best competitor and the AUPR of HetSheaf is 98.24 % compared to 97.16 of HetSheaf-NSD. On MovieLens, a similar story emerges, but HetSheaf performs only slightly better than HetSheaf-NSD. The power of the sheaf is demonstrated by the fact that the two best-performing models for link prediction, HetSheaf-NSD and HetSheaf, are both sheaf architectures.

5.3 Model Analysis

Sheaf predictor ablation study. For node classification, all the sheaf modifications perform better or similar compared to the vanilla feature concatenation sheaf learners used by HetSheaf-NSD, demonstrating that these modifications are useful for processing heterogeneous data. This suggests that the type information encodes vital information required for heterogeneous tasks; it is also visible in the performance gap between the homogeneous and heterogeneous GNNs. For these particular datasets, Table 3 suggests that the type information is more informative than the node features as sheaves that learn the restriction maps using just the type information (HetSheaf-NT and HetSheaf-ET) outperform HetSheaf-NSD.

Table 4 repeats the ablation studies for the link prediction datasets. In both datasets, the heterogeneous sheaf learners perform comparably to or outperform the base HetSheaf-NSD implementation. In LastFM, they perform better than HetSheaf-NSD, and on MovieLens embedding, just the type information performs 0.02 % to 0.05 % lower than HetSheaf-NSD. This again illustrates the importance of the type information, which appears to be more informative than the local features. Interestingly, HetSheaf-NT, which predicts the restriction maps using only the node type information, performs the best on LastFM. This is likely an artefact of the dataset as each edge type is *type specific*. That is, they only connect nodes of certain types. As we attempt to predict the edges of a certain type, it is natural that including only the node type information performs the best, as the model must only learn which node types define that edge type. A more interesting test could use a dataset in which an edge type may connect different node types.

Effect of restriction map type. Table 3 also shows the impact of the restriction map type on each sheaf model’s performance for node classification tasks. Across the board, general restriction maps perform the best, with orthogonal restriction maps performing the worst. This is despite the theoretical benefits of orthogonal restriction maps because of their connection with parallel transport. The most likely reason for better performance with general restriction maps is that they are more expressive and can encode more complex interactions in the edge stalks compared to the other methods. The poor performance of orthogonal restriction maps is due to the transformations they represent not being sufficiently complex to encode the structure and interactions in the heterogeneous graph datasets. Interestingly, this is in contrast to Bodnar et al. [4], which found that orthogonal restriction maps performed better on their datasets. This suggests that the best restriction map properties depend on the particular task.

We may repeat this for the link prediction tasks. Table 4 shows the effect of each restriction map type on the performance of the sheaf architecture. Unlike the node classification results above, the restriction maps appear to have a much smaller effect on the overall model performance. Aligning with both Bodnar et al. [4], Duta et al. [12], the diagonal restriction maps perform well on HetSheaf-NSD. The results for the heterogeneous sheaf learners are more mixed, but generally, the general restriction maps seem to perform slightly better than either diagonal or orthogonal restriction maps. However, this difference is 0.5 % compared to the performance gap of 1 % to 2 % observed with general restriction maps for node classification.

Table 4: **Restriction map and sheaf predictor ablation study for heterogeneous link prediction.** The highest performing restriction map type for each sheaf learner is highlighted, and the highest performing sheaf learner is shown in **bold**.

	LastFM		MovieLens	
	AUPR	AUROC	AUPR	AUROC
O(d)-NSD	96.91 \pm 0.02	96.35 \pm 0.21	99.62 \pm 0.06	99.52 \pm 0.05
Diag-NSD	97.16 \pm 0.19	96.58 \pm 0.18	99.66 \pm 0.04	99.57 \pm 0.03
Gen-NSD	97.01 \pm 0.13	96.44 \pm 0.18	99.66 \pm 0.06	99.55 \pm 0.07
O(d)-TE (ours)	97.70 \pm 0.61	97.23 \pm 0.63	99.58 \pm 0.05	99.49 \pm 0.06
Diag-TE (ours)	97.70 \pm 0.55	97.21 \pm 0.64	99.63 \pm 0.08	99.53 \pm 0.08
Gen-TE (ours)	97.71 \pm 0.52	97.17 \pm 0.55	99.65 \pm 0.03	99.57 \pm 0.04
O(d)-ensemble (ours)	97.15 \pm 0.11	96.46 \pm 0.13	99.61 \pm 0.08	99.51 \pm 0.08
Diag-ensemble (ours)	97.93 \pm 0.25	97.35 \pm 0.28	99.68 \pm 0.04	99.59 \pm 0.04
Gen-ensemble (ours)	98.21 \pm 0.15	97.71 \pm 0.18	99.66 \pm 0.06	99.57 \pm 0.05
O(d)-NE (ours)	97.90 \pm 0.68	97.43 \pm 0.07	99.62 \pm 0.05	99.52 \pm 0.04
Diag-NE (ours)	97.62 \pm 0.51	97.13 \pm 0.53	99.66 \pm 0.05	99.56 \pm 0.06
Gen-NE (ours)	98.00 \pm 0.46	97.51 \pm 0.51	99.66 \pm 0.04	99.57 \pm 0.04
O(d)-EE (ours)	96.98 \pm 0.17	96.42 \pm 0.17	99.59 \pm 0.07	99.50 \pm 0.06
Diag-EE (ours)	97.40 \pm 0.49	96.84 \pm 0.52	99.67 \pm 0.05	99.57 \pm 0.05
Gen-EE (ours)	97.51 \pm 0.44	96.91 \pm 0.52	99.63 \pm 0.05	99.51 \pm 0.06
O(d)-NT (ours)	98.24 \pm 0.13	97.80 \pm 0.18	99.61 \pm 0.03	99.52 \pm 0.03
Diag-NT (ours)	97.87 \pm 0.36	97.50 \pm 0.39	99.60 \pm 0.05	99.51 \pm 0.05
Gen-NT (ours)	98.15 \pm 0.19	97.69 \pm 0.25	99.61 \pm 0.06	99.52 \pm 0.06
O(d)-ET (ours)	96.80 \pm 0.29	96.26 \pm 0.24	99.56 \pm 0.05	99.45 \pm 0.04
Diag-ET (ours)	97.70 \pm 0.19	97.16 \pm 0.18	99.62 \pm 0.06	99.54 \pm 0.05
Gen-ET (ours)	97.84 \pm 0.32	97.26 \pm 0.30	99.64 \pm 0.03	99.54 \pm 0.03

Computational overhead. Table 7 shows the computational overhead of HETSHEAF in terms of the total runtime and the number of trainable parameters. The baseline architectures that performed best across all datasets were HGT and R-GCN, with the largest sheaf architecture (HetSheaf-ensemble) being, on average, 111x smaller than R-GCN and 17x smaller than HGT in terms of the number of model parameters across all datasets. This demonstrates the benefit of these sheaves as they either exceed or perform similarly to existing approaches with a substantially smaller model architecture with reduced memory overhead. It is important to note that the sheaf architectures were implemented by adapting the original HetSheaf-NSD implementation [4]. So, the sheaf implementations could be more computationally efficient, while the baseline implementations are from PyG [14] and are substantially more optimised.

6 Conclusion

In this paper, we introduce HETSHEAF, a framework for creating heterogeneous sheaf neural networks. We propose a series of heterogeneous sheaf predictors which explicitly account for the type information present in heterogeneous settings and provide a natural way to model a graph’s heterogeneity. This novel framework generalises existing sheaf architectures, and we empirically demonstrate they outperform existing methods on several datasets, whilst being substantially more efficient in terms of parameters. Our heterogeneous sheaf predictors establish a general framework that may be applied to any existing or future sheaf architectures. As underlying sheaf GNNs improve, performance on heterogeneous data will likely improve alongside it. The framework presented in this paper can also be easily lifted to other domains, such as hypergraphs and more general topological domains [see 30, 19].

Acknowledgments

This work was performed using resources provided by the Cambridge Service for Data Driven Discovery (CSD3) operated by the University of Cambridge Research Computing Service (www.csd3.cam.ac.uk), provided by Dell EMC and Intel using Tier-2 funding from the Engineering and Physical Sciences Research Council (capital grant EP/T022159/1), and DiRAC funding from the Science and Technology Facilities Council (www.dirac.ac.uk).

References

- [1] Uri Alon and Eran Yahav. On the bottleneck of graph neural networks and its practical implications. In *International Conference on Learning Representations*, 2021.
- [2] Federico Barbero, Cristian Bodnar, Haitz Sáez de Ocáriz Borde, Michael Bronstein, Petar Veličković, and Pietro Liò. Sheaf Neural Networks with Connection Laplacians. In *Proceedings of Topological, Algebraic, and Geometric Learning Workshops 2022*, pages 28–36. PMLR, November 2022.
- [3] Federico Barbero, Cristian Bodnar, Haitz Sáez de Ocáriz Borde, and Pietro Lio. Sheaf Attention Networks. In *NeurIPS 2022 Workshop on Symmetry and Geometry in Neural Representations*, November 2022.
- [4] Cristian Bodnar, Francesco Di Giovanni, Benjamin Paul Chamberlain, Pietro Lio, and Michael M. Bronstein. Neural Sheaf Diffusion: A Topological Perspective on Heterophily and Oversmoothing in GNNs. In *NeurIPS 2022*, May 2022.
- [5] Chen Cai and Yusu Wang. A Note on Over-Smoothing for Graph Neural Networks, June 2020. arXiv:2006.13318.
- [6] Yukuo Cen, Xu Zou, Jianwei Zhang, Hongxia Yang, Jingren Zhou, and Jie Tang. Representation Learning for Attributed Multiplex Heterogeneous Network. In *Proceedings of the 25th ACM SIGKDD International Conference on Knowledge Discovery & Data Mining, KDD '19*, pages 1358–1368, New York, NY, USA, July 2019. Association for Computing Machinery. ISBN 978-1-4503-6201-6.
- [7] Ben Chamberlain, James Rowbottom, Maria I. Gorinova, Michael Bronstein, Stefan Webb, and Emanuele Rossi. GRAND: Graph Neural Diffusion. In *Proceedings of the 38th International Conference on Machine Learning*, pages 1407–1418. PMLR, July 2021.
- [8] Gabriele Corso, Luca Cavalleri, Dominique Beaini, Pietro Liò, and Petar Veličković. Principal neighbourhood aggregation for graph nets. In *Advances in Neural Information Processing Systems*, 2020.
- [9] Justin Curry. Sheaves, Cosheaves and Applications, December 2014. arXiv:1303.3255.
- [10] Michaël Defferrard, Xavier Bresson, and Pierre Vandergheynst. Convolutional Neural Networks on Graphs with Fast Localized Spectral Filtering. In *Advances in Neural Information Processing Systems*, volume 29. Curran Associates, Inc., 2016.
- [11] Yuxiao Dong, Nitesh V. Chawla, and Ananthram Swami. metapath2vec: Scalable Representation Learning for Heterogeneous Networks. In *Proceedings of the 23rd ACM SIGKDD International Conference on Knowledge Discovery and Data Mining, KDD '17*, pages 135–144, New York, NY, USA, August 2017. Association for Computing Machinery. ISBN 978-1-4503-4887-4.
- [12] Iulia Duta, Giulia Cassarà, Fabrizio Silvestri, and Pietro Lio. Sheaf Hypergraph Networks. In *Thirty-seventh Conference on Neural Information Processing Systems, NeurIPS 2023*, November 2023.
- [13] Wenqi Fan, Yao Ma, Qing Li, Yuan He, Eric Zhao, Jiliang Tang, and Dawei Yin. Graph Neural Networks for Social Recommendation. In *The World Wide Web Conference*, pages 417–426, San Francisco CA USA, May 2019. ACM. ISBN 978-1-4503-6674-8.
- [14] Matthias Fey and Jan Eric Lenssen. Fast Graph Representation Learning with PyTorch Geometric, April 2019. arXiv:1903.02428.
- [15] Alex Fout, Jonathon Byrd, Basir Shariat, and Asa Ben-Hur. Protein Interface Prediction using Graph Convolutional Networks. In *Advances in Neural Information Processing Systems*, volume 30. Curran Associates, Inc., 2017.

- [16] Xinyu Fu, Jiani Zhang, Ziqiao Meng, and Irwin King. MAGNN: Metapath Aggregated Graph Neural Network for Heterogeneous Graph Embedding. In *Proceedings of The Web Conference 2020*, pages 2331–2341, April 2020.
- [17] Justin Gilmer, Samuel S. Schoenholz, Patrick F. Riley, Oriol Vinyals, and George E. Dahl. Neural Message Passing for Quantum Chemistry, June 2017. arXiv:1704.01212.
- [18] Shengnan Guo, Youfang Lin, Ning Feng, Chao Song, and Huaiyu Wan. Attention Based Spatial-Temporal Graph Convolutional Networks for Traffic Flow Forecasting. *Proceedings of the AAAI Conference on Artificial Intelligence*, 33(01):922–929, July 2019. ISSN 2374-3468.
- [19] Mustafa Hajij, Ghada Zamzmi, Theodore Papamarkou, Nina Miolane, Aldo Guzmán-Sáenz, Karthikeyan Natesan Ramamurthy, Tolga Birdal, Tamal K. Dey, Soham Mukherjee, Shreyas N. Samaga, Neal Livesay, Robin Walters, Paul Rosen, and Michael T. Schaub. Topological Deep Learning: Going Beyond Graph Data, May 2023. arXiv:2206.00606.
- [20] William L. Hamilton. *Graph Representation Learning*. Synthesis Lectures on Artificial Intelligence and Machine Learning. Springer International Publishing, Cham, 2020. ISBN 978-3-031-00460-5.
- [21] Jakob Hansen and Robert Ghrist. Opinion Dynamics on Discourse Sheaves, May 2020. arXiv:2005.12798.
- [22] Yu He, Cristian Bodnar, and Pietro Lio. Sheaf-based Positional Encodings for Graph Neural Networks. In *NeurIPS 2023 Workshop on Symmetry and Geometry in Neural Representations*, November 2023.
- [23] Ziniu Hu, Yuxiao Dong, Kuansan Wang, Kai-Wei Chang, and Yizhou Sun. GPT-GNN: Generative Pre-Training of Graph Neural Networks. In *Proceedings of the 26th ACM SIGKDD International Conference on Knowledge Discovery & Data Mining, KDD '20*, pages 1857–1867, New York, NY, USA, August 2020. Association for Computing Machinery. ISBN 978-1-4503-7998-4.
- [24] Ziniu Hu, Yuxiao Dong, Kuansan Wang, and Yizhou Sun. Heterogeneous Graph Transformer, March 2020. arXiv:2003.01332.
- [25] Thomas N. Kipf and Max Welling. Semi-Supervised Classification with Graph Convolutional Networks. In *ICLR 2016*, November 2016.
- [26] Chang Li and Dan Goldwasser. Encoding Social Information with Graph Convolutional Networks for Political Perspective Detection in News Media. In Anna Korhonen, David Traum, and Lluís Màrquez, editors, *Proceedings of the 57th Annual Meeting of the Association for Computational Linguistics*, pages 2594–2604, Florence, Italy, July 2019. Association for Computational Linguistics.
- [27] Yujia Li, Daniel Tarlow, Marc Brockschmidt, and Richard Zemel. Gated Graph Sequence Neural Networks, September 2017. arXiv:1511.05493.
- [28] Qingsong Lv, Ming Ding, Qiang Liu, Yuxiang Chen, Wenzheng Feng, Siming He, Chang Zhou, Jianguo Jiang, Yuxiao Dong, and Jie Tang. Are we really making much progress? Revisiting, benchmarking and refining heterogeneous graph neural networks. In *Proceedings of the 27th ACM SIGKDD Conference on Knowledge Discovery & Data Mining, KDD '21*, pages 1150–1160, New York, NY, USA, August 2021. Association for Computing Machinery. ISBN 978-1-4503-8332-5.
- [29] Anton Obukhov. Efficient householder transformation in pytorch, 2021. URL www.github.com/toshas/torch-householder. Version: 1.0.1, DOI: 10.5281/zenodo.5068733.
- [30] Mathilde Papillon, Sophia Sanborn, Mustafa Hajij, and Nina Miolane. Architectures of Topological Deep Learning: A Survey on Topological Neural Networks, August 2023. arXiv:2304.10031.
- [31] Antonio Purificato, Giulia Cassarà, Federico Siciliano, Pietro Liò, and Fabrizio Silvestri. Sheaf4Rec: Sheaf Neural Networks for Graph-based Recommender Systems, March 2024. arXiv:2304.09097.
- [32] Jiezhong Qiu, Jian Tang, Hao Ma, Yuxiao Dong, Kuansan Wang, and Jie Tang. DeepInf: Social Influence Prediction with Deep Learning. In *Proceedings of the 24th ACM SIGKDD*

- International Conference on Knowledge Discovery & Data Mining*, KDD '18, pages 2110–2119, New York, NY, USA, July 2018. Association for Computing Machinery. ISBN 978-1-4503-5552-0.
- [33] Daniel Rosiak. *Sheaf theory through examples*. MIT Press, Cambridge, Massachusetts, 1st ed. edition, 2022. ISBN 978-0-262-36237-5.
 - [34] Michael Schlichtkrull, Thomas N. Kipf, Peter Bloem, Rianne van den Berg, Ivan Titov, and Max Welling. Modeling Relational Data with Graph Convolutional Networks, October 2017. arXiv:1703.06103.
 - [35] Michael Schlichtkrull, Thomas N. Kipf, Peter Bloem, Rianne van den Berg, Ivan Titov, and Max Welling. Modeling Relational Data with Graph Convolutional Networks. In Aldo Gangemi, Roberto Navigli, Maria-Esther Vidal, Pascal Hitzler, Raphaël Troncy, Laura Hollink, Anna Tordai, and Mehwish Alam, editors, *The Semantic Web*, pages 593–607, Cham, 2018. Springer International Publishing. ISBN 978-3-319-93417-4.
 - [36] Allen Dudley Shepard. *A Cellular Description of the Derived Category of a Stratified Space*. PhD thesis, Brown University, 1985.
 - [37] Jasper Snoek, Hugo Larochelle, and Ryan P. Adams. Practical Bayesian Optimization of Machine Learning Algorithms, August 2012. arXiv:1206.2944.
 - [38] Yizhou Sun and Jiawei Han. *Mining Heterogeneous Information Networks: Principles and Methodologies*. Synthesis Lectures on Data Mining and Knowledge Discovery. Springer International Publishing, Cham, 2012. ISBN 978-3-031-01902-9.
 - [39] Yizhou Sun, Jiawei Han, Xifeng Yan, Philip S. Yu, and Tianyi Wu. PathSim: meta path-based top-K similarity search in heterogeneous information networks. *Proc. VLDB Endow.*, 4(11): 992–1003, August 2011. ISSN 2150-8097.
 - [40] Ashish Vaswani, Noam Shazeer, Niki Parmar, Jakob Uszkoreit, Llion Jones, Aidan N Gomez, Łukasz Kaiser, and Illia Polosukhin. Attention is All you Need. In *Advances in Neural Information Processing Systems*, volume 30. Curran Associates, Inc., 2017.
 - [41] Petar Veličković, Guillem Cucurull, Arantxa Casanova, Adriana Romero, Pietro Liò, and Yoshua Bengio. Graph Attention Networks. In *ICLR 2018*, February 2018.
 - [42] Petar Veličković, William Fedus, William L. Hamilton, Pietro Liò, Yoshua Bengio, and R. De-von Hjelm. Deep Graph Infomax. In *International Conference on Learning Representations*, September 2018.
 - [43] Xiao Wang, Houye Ji, Chuan Shi, Bai Wang, Peng Cui, P. Yu, and Yanfang Ye. Heterogeneous Graph Attention Network, March 2019. arXiv:1903.07293.
 - [44] Xiao Wang, Houye Ji, Chuan Shi, Bai Wang, Yanfang Ye, Peng Cui, and Philip S Yu. Heterogeneous Graph Attention Network. In *The World Wide Web Conference, WWW '19*, pages 2022–2032, New York, NY, USA, May 2019. Association for Computing Machinery. ISBN 978-1-4503-6674-8.
 - [45] Keyulu Xu, Chengtao Li, Yonglong Tian, Tomohiro Sonobe, Ken-ichi Kawarabayashi, and Stefanie Jegelka. Representation Learning on Graphs with Jumping Knowledge Networks. In *Proceedings of the 35th International Conference on Machine Learning*, pages 5453–5462. PMLR, July 2018.
 - [46] Bishan Yang, Wen-tau Yih, Xiaodong He, Jianfeng Gao, and Li Deng. Embedding Entities and Relations for Learning and Inference in Knowledge Bases, August 2015. arXiv:1412.6575.
 - [47] Carl Yang, Aditya Pal, Andrew Zhai, Nikil Pancha, Jiawei Han, Charles Rosenberg, and Jure Leskovec. MultiSage: Empowering GCN with Contextualized Multi-Embeddings on Web-Scale Multipartite Networks. In *Proceedings of the 26th ACM SIGKDD International Conference on Knowledge Discovery & Data Mining, KDD '20*, pages 2434–2443, New York, NY, USA, August 2020. Association for Computing Machinery. ISBN 978-1-4503-7998-4.
 - [48] Carl Yang, Yuxin Xiao, Yu Zhang, Yizhou Sun, and Jiawei Han. Heterogeneous Network Representation Learning: A Unified Framework With Survey and Benchmark. *IEEE Trans. on Knowl. and Data Eng.*, 34(10):4854–4873, October 2022. ISSN 1041-4347.

- [49] Gang Yang, Xiaofeng Zhang, and Yueping Li. Session-Based Recommendation with Graph Neural Networks for Repeat Consumption. In *Proceedings of the 2020 9th International Conference on Computing and Pattern Recognition, ICCPR '20*, pages 519–524, New York, NY, USA, January 2021. Association for Computing Machinery. ISBN 978-1-4503-8783-5.
- [50] Seongjun Yun, Minbyul Jeong, Raehyun Kim, Jaewoo Kang, and Hyunwoo J Kim. Graph Transformer Networks. In *Advances in Neural Information Processing Systems*, volume 32. Curran Associates, Inc., 2019.
- [51] Chuxu Zhang, Dongjin Song, Chao Huang, Ananthram Swami, and Nitesh V. Chawla. Heterogeneous Graph Neural Network. In *Proceedings of the 25th ACM SIGKDD International Conference on Knowledge Discovery & Data Mining, KDD '19*, pages 793–803, New York, NY, USA, July 2019. Association for Computing Machinery. ISBN 978-1-4503-6201-6.
- [52] Tianyu Zhao, Cheng Yang, Yibo Li, Quan Gan, Zhenyi Wang, Fengqi Liang, Huan Zhao, Yingxia Shao, Xiao Wang, and Chuan Shi. Space4HGNN: A Novel, Modularized and Reproducible Platform to Evaluate Heterogeneous Graph Neural Network. In *Proceedings of the 45th International ACM SIGIR Conference on Research and Development in Information Retrieval, SIGIR '22*, pages 2776–2789, New York, NY, USA, July 2022. Association for Computing Machinery. ISBN 978-1-4503-8732-3.
- [53] Ziang Zhou, Jieming Shi, Renchi Yang, Yuanhang Zou, and Qing Li. SlotGAT: Slot-based Message Passing for Heterogeneous Graphs. In *Proceedings of the 40th International Conference on Machine Learning*, pages 42644–42657. PMLR, July 2023.
- [54] Shichao Zhu, Chuan Zhou, Shirui Pan, Xingquan Zhu, and Bin Wang. Relation Structure-Aware Heterogeneous Graph Neural Network. In *2019 IEEE International Conference on Data Mining (ICDM)*, pages 1534–1539, November 2019.

A Appendix

A.1 Experimental Details

A.1.1 Datasets

Table 5: **Statistics of benchmark datasets.**

<i>Node classification</i>	# Nodes	# Node types	# Edges	# Edge types	Target	# Classes
DBLP	26,128	4	239,566	6	author	4
IMDB	21,420	4	86,642	6	movie	5
ACM	10,942	4	547,872	8	paper	3
<i>Link prediction</i>					Target	
LastFM	20,612	3	141,521	3	user-artist	
MovieLens	10,352	2	201,672	2	user-movie	

Each of the datasets used is publicly available as part of the Heterogeneous Graph Benchmark (HGB)² first introduced by Lv et al. [28]. We provide brief descriptions of each dataset.

- **DBLP**³ is a citation graph based on the DBLP computer science bibliographic database. It has four node types: authors, papers, venues and terms. The six edge types include paper-author, paper-venue, paper-term and author-venue. The target is to predict the class label of authors based on their research area: databases, data mining, AI or information retrieval.
- **IMDB**⁴ is an information graph containing movie data. The four node types are movies, directors, actors and keywords. The six edge types include movie-director, movie-actor and movie-keyword. Movies are classified based on their genre: action, comedy, drama,

²<https://www.biendata.xyz/hgb/>

³<https://web.cs.ucla.edu/~yzsun/data/>

⁴<https://www.kaggle.com/datasets/karrrimba/movie-metadatasv>

romance and thriller. Each movie can have multiple genres, i.e., a multi-label node classification task.

- **ACM** [44] is a citation graph containing node types of authors, papers, terms and subjects. The edge types include paper-cite-paper, paper-author, paper-subject and paper-term. The target is to predict each paper’s category: databases, wireless communication, or data mining.
- **LastFM**⁵ is a knowlege graph generated from an online music website. The three node types are user, artist, and tags with edge types of user-artist, user-user and artist-tag. The link prediction task aims to predict edges between users and artists.
- **MovieLens**⁶ is a heterogeneous rating graph from the MovieLens website and consists of two node types: movie and user. The task is to predict whether or not a user recommends a movie.

A.1.2 Model Hyperparameters

Table 6 shows the search space used to optimise the model hyperparameters. For each model, 200 hyperparameter sweeps were run using Bayesian optimisation [37] to maximise the validation accuracy.

Table 6: **Hyperparameter search space.**

Hyperparameter	Search space
Sheaf type	$\{\text{general}, O(d), \text{diagonal}\}$
Sheaf learner	$\{\text{NSD}, \text{TE}, \text{EE}, \text{NE}, \text{types}, \text{NT}, \text{ET}\}$
d	$\{2, 3, 4, 5\}$
# Layers	$\{2, 3, 4, 5, 6, 7, 8\}$
input_dropout	$[0, 0.9]$
dropout	$[0, 0.9]$
initial_dropout	$[0, 0.9]$
Learning rate	$\{1, 5\} \times \{10^{-5}, 10^{-4}, 10^{-3}, 10^{-2}\}$
Weight decay	$\{1, 5\} \times \{10^{-5}, 10^{-4}, 10^{-3}\}$

A.2 Implementation Details

A.2.1 Downstream Decoder Architecture & Loss Functions

Node classification. After the Sheaf GNN processes the graph, the final node embeddings are fed into an MLP to generate the final classification logits. For multiclass tasks, we use a softmax activation with cross-entropy loss, and for multilabel classification, we use a sigmoid activation with binary cross-entropy loss.

Link prediction. For each node pair u, v and relation type r , the model outputs the score

$$P(u \sim_r v) = \text{Decoder}(\mathbf{H}_u, \mathbf{H}_v) \quad (13)$$

which gives the probability that u and v are connected by a relation of type r . As this is a binary classification task, the binary cross entropy loss is used.

The decoder can take several forms. A dot product decoder first computes the dot product and then applies a sigmoid activation function: $\text{Decoder}(\mathbf{H}_u, \mathbf{H}_v) = \sigma(\langle \mathbf{H}_u, \mathbf{H}_v \rangle)$.

DistMult [46] calculates the bi-linear form $\text{Decoder}(\mathbf{H}_u, \mathbf{H}_v) = \sigma(\mathbf{H}_u^\top \mathbf{W}_{\psi(u,v)} \mathbf{H}_v)$ between \mathbf{H}_u and \mathbf{H}_v where $\mathbf{W}_{\psi(u,v)} \in \mathbb{R}^{d_L \times d_L}$ is a learnable weight matrix for each edge type $\psi(u, v)$.

A concat decoder concatenates the two representations together, applies a one-layer MLP and finally applies a sigmoid activation function: $\text{Decoder}(\mathbf{H}_u, \mathbf{H}_v) = \sigma(\text{MLP}(\mathbf{H}_u \parallel \mathbf{H}_v))$. Similar to Lv et al. [28], we leave the choice of the decoder as a hyperparameter.

⁵<https://grouplens.org/datasets/hetrec-2011/>

⁶<https://movielens.org/>

A.2.2 Restriction Map Implementation

Each restriction map is computed $d \times d$ block matrix and parameterised by the matrix-valued function $\Phi(\mathbf{x}_u, \mathbf{x}_v, \phi(u), \phi(v), \psi(e))$. We briefly describe how restriction maps of each type are computed.

Diagonal restriction maps. For the diagonal restriction maps, the MLP outputs d elements, which are used to define the diagonal of the restriction map.

General restriction maps. For general restriction maps, the MLP outputs d^2 elements that are then rearranged to form a $d \times d$ matrix representing the restriction map.

Orthogonal restriction maps. For orthogonal restriction maps, MLP outputs $\lfloor \frac{d(d-1)}{2} \rfloor$ elements, and then the Torch Householder library [29] is used to generate a $d \times d$ orthogonal restriction map.

Low rank restriction maps. To predict a rank r restriction map, the MLP outputs $2dr + d$ elements that are rearranged into two matrices $\mathbf{A}, \mathbf{B} \in \mathbb{R}^{d \times r}$ and a vector $\mathbf{c} \in \mathbb{R}^d$. The final restriction map is computed as $\mathbf{AB}^\top + \text{diag}(\mathbf{c})$.

A.3 HETSHEAF computational overhead

Table 7 shows HETSHEAF’s average run time and model size compared to baseline architectures. The runtime is provided for completeness and to give an indication of the computational requirements of HETSHEAF.

Table 7: **HETSHEAF computational overhead on node classification tasks.** The highest performing baseline architectures are highlighted with the highest performing HETSHEAF model shown in bold.

	ACM		DBLP		IMDB	
	Runtime (s)	# params	Runtime (s)	# params	Runtime (s)	# params
GAT	111.1	8.6M	32.5	13.4M	22.7	11.9M
GCN	17.9	619K	10.4	1.2M	7.9	1.0M
HAN	28.9	2.2M	18.5	1.9M	15.8	3.4M
R-GCN	22.1	43M	30.3	87.8M	25.9	72.1M
HGT	1025.8	7.2M	648.3	6.2M	939.9	10.5M
HetSheaf-NSD	47.6	155K	73.3	1.7M	40.5	1.6M
HetSheaf-TE (ours)	44.7	155K	79.1	1.7M	40.1	1.6M
HetSheaf-ensemble (ours)	55.7	174K	83.2	1.8M	44.9	1.9M
HetSheaf-NE (ours)	47.3	155K	89.6	1.7M	12.0	1.1M
HetSheaf-EE (ours)	49.6	155K	85.9	1.7M	41.8	1.6M
HetSheaf-NT (ours)	42.0	154K	82.4	1.7M	38.6	1.6M
HetSheaf-ET (ours)	45.1	154K	80.5	1.7M	39.8	1.6M